Radboud University Nijmegen

Department of Theoretical High Energy Physics

Master's thesis

The link between a vacuum diagram and the renormalization group equation

Author:
Daphne van den Elzen

Supervisor:
Prof. dr. Wim Beenakker

September 1, 2016

Contents

1 Introduction

What exactly is the vacuum? It seems a rather simple question, but when zooming in on this subject it actually turns out to be a pretty complex one. The most obvious definition of the vacuum is empty space; the absence of matter and radiation. When looking at it from the angle of quantum field theory however, the notion of empty space is replaced with that of a vacuum state. It is defined to be the lowest energy state, also called the ground state, of all fundamental fields. This energy isn't zero, as expected from classical mechanics, but it has a value due to zero-point fluctuations of the fields made possible by quantum mechanics. Summing all contributions of zero-point energies leads to an infinite vacuum energy. To make sense of a quantum field theory we need to remove this infinity. This is done by renormalizing the theory.

The vacuum energy density predicted by quantum field theory does not match that observed in cosmology. There is actually much less energy present in the vacuum than one would expect from quantum field theory. This is known as the cosmological constant problem and is the motivation for our research. Following up on previous research we will zoom in on the processes that contribute to the vacuum energy and on the renormalization procedure. We will investigate if there is a link between the so-called vacuum diagrams and the renormalization group equation. We will also discuss the effect of assuming that transitions between states in the renormalization group equation are abrupt.

Before diving into our research we will look at the theoretical background in chapter 2. We will explore where the vacuum energy comes from, examine the cosmological constant problem and look into the previous research in this field. We will also provide background information needed to start our own research. In chapter 3 we will do the calculations needed to answer our research question. We will calculate the vacuum diagrams and compare the result to the renormalization group equation. In chapter 4 we will conclude and discuss our results.

In this thesis we will use natural units ($\hbar = \mathrm{c} = 1$), the metric for flat spacetime $g_{\mu\nu} = \mathrm{diag}(1,-1,-1,-1)$ and the Einstein summation convention, unless mentioned otherwise.

2 Theoretical context

2.1 The cosmological constant problem

The motivation for our research lies in the cosmological constant problem, which is regarded as a fundamental problem in modern physics. The cosmological constant problem arises at the intersection between quantum field theory and general relativity. The cosmological constant is a homogeneous energy density that spans the whole universe. The problem is that there is a huge gap between the experimentally determined value of the cosmological constant and the theoretically calculated one.

From the perspective of general relativity we rely on the modified Einstein field equations [1], which describe the curvature of spacetime by matter and energy:

$$R_{\mu\nu} - \frac{1}{2} R g_{\mu\nu} + \Lambda g_{\mu\nu} = -8\pi G T_{\mu\nu} \ ,$$

with the energy-momentum tensor $T_{\mu\nu}$, Newton's gravitational constant G, Ricci tensor $R_{\mu\nu}$, scalar curvature $R = g^{\rho\sigma} R_{\rho\sigma}$ and cosmological constant Λ. The right hand side of the equation describes the matter and energy in the universe, whereas the left hand side describes the structure of spacetime for the vacuum. In the context of the cosmological constant problem the Λ-term is commonly moved onto the right-hand side of the equation. Then it can be viewed as the energy density and pressure of empty space:

$$T^{eff}_{\mu\nu} \equiv T_{\mu\nu} + \frac{\Lambda g_{\mu\nu}}{8\pi G} \quad \Rightarrow \quad T^{vac}_{\mu\nu} = \frac{\Lambda g_{\mu\nu}}{8\pi G} \ .$$

Such a term therefore constitutes the contribution of the vacuum to the curvature. For a positive cosmological constant the energy density of the vacuum is positive and the associated pressure negative, resulting in an accelerated expansion of empty space, as seems to be supported by experiment. Solar system observations, galactic observations and large scale cosmology have led to the following value of the cosmological constant: $\Lambda \approx 10^{-52}\ m^{-2}$ [2].

The existence of the cosmological constant is also predicted by quantum field theory, where it enters as a form of vacuum energy. In general, when quantizing a theory one considers the fluctuations of fields around minima of the classical action. These fluctuations define a set of harmonic oscillators, to which one applies the quantization procedure [3]. This also holds for quantum field theory; all fundamental fields are treated as quantized harmonic oscillators in every point in space and time. Each quantized harmonic oscillator has a non-vanishing zero-point energy in contrast to a classical harmonic oscillator, which can be completely at rest and have zero energy. This gives rise to a field contribution to the zero-point energy density of the form

$$\int_{-\infty}^{\infty} \frac{d\vec{p}}{(2\pi)^3}\ \omega_{\vec{p}} \ ,$$

with $\omega_{\vec{p}} \equiv \sqrt{\vec{p}^2 + m^2}$ [1]. It is infinite due to the fact that the integration is over all values of momentum $\vec{p}$. This type of infinity is called an ultraviolet

divergence, because it originates from taking the limit $|\vec{p}| \to \infty$. Therewith we assume that quantum field theory is valid up to arbitrary high energies, which is not the case. It is often assumed that the theory breaks down at the Planck scale $\Lambda_P = 10^{19}$ GeV (the energy scale at which gravitation needs to be accounted for). But also when using this energy cutoff the vacuum energy density exceeds the cosmologically observed value by about 120 orders of magnitude [2]. Another way to approach vacuum energy is from the particle perspective. Particles are derived quantities resulting from quantization of the more fundamental fields. From the particle view the vacuum energy is caused by so-called vacuum bubbles. These are Feynman diagrams without external lines. Vacuum bubbles are the result of virtual particles; particles that don't meet the energy-momentum relation $m^2c^4 = E^2 - \vec{p}^2c^2$. Due to the time-energy uncertainty relation $\Delta E \Delta t \geq \mathcal{O}(\hbar)$ energetic particles can be excited from the vacuum for a short amount of time. Summing over all possible vacuum bubbles, as imposed by quantum field theory, results in the infinity as mentioned before.

2.2 Previous research on the cosmological constant problem

Previous research in this field [4] has tried to bridge the gap between theory and experiment, with some success. It was discovered that only certain terms in the Lagrangian density of a quantum field theory contribute to the cosmological constant. The Lagrangian density $\mathcal{L}$, often referred to as the Lagrangian, describes the properties of a system in a field theory [1]. In the relativistic case the Lagrangian depends on fields $\phi_j(x)$ and the corresponding four-velocities $\partial_\mu \phi_j(x)$, where the fields $\phi_j(x)$ depend on the spacetime four-vector x and j labels the fields. Given a Lagrangian the equations of motion for a field are given by the so-called Euler-Lagrange equation:

$$\partial_\mu \left(\frac{\partial \mathcal{L}}{\partial(\partial_\mu \phi_j)} \right) = \frac{\partial \mathcal{L}}{\partial \phi_j} \, .$$

Relativistic field theories have a symmetry under continuous translations in space and time. According to Noether's theorem every continuous symmetry comes with a conserved current. In this case the conserved currents are given by the energy-momentum tensor:

$$T^{\mu\nu} \equiv \left(\frac{\partial \mathcal{L}}{\partial(\partial_\mu \phi_j)} \right) \partial^\nu \phi_j - g^{\mu\nu} \mathcal{L} \, .$$

It describes the current density of the ν^{th} component of the momentum four-vector p^ν in the direction of the μ^{th} component of the spacetime four-vector x^μ. Or in other words: it describes the density and flux of energy and momentum in spacetime.

Now that we know what the Lagrangian and energy-momentum tensor are, we can look at the result of previous research. It was determined which terms in an arbitrary Lagrangian contribute to the quantum mechanical contribution to the cosmological constant:

$$\frac{1}{4} \left\langle \Omega \left| \hat{T}^\rho_\rho \right| \Omega \right\rangle = \frac{1}{4} \left(\sum_{\hat{f}} \left\langle \Omega \left| (d_{\hat{f}} + 1) \frac{\partial \hat{\mathcal{L}}}{\partial(\partial_\rho \hat{f})} \partial_\rho \hat{f} + d_{\hat{f}} \frac{\partial \hat{\mathcal{L}}}{\partial \hat{f}} \hat{f} \right| \Omega \right\rangle - 4 \left\langle \Omega \left| \hat{\mathcal{L}} \right| \Omega \right\rangle \right) \, ,$$

with ground state $|\Omega\rangle$, fields $\hat{f}$ and $d_{\hat{f}}$ the mass dimension of field $\hat{f}$. The function between the brackets counts the number of fields and the number of derivatives of fields in all terms of the Lagrangian, multiplies them with their mass dimension and subtracts 4. As the Lagrangian has mass dimension 4 only terms with a dimensionful coupling constant survive. What we are left with is:

$$\frac{1}{4}\left\langle \Omega \left| \hat{T}^{\rho}_{\rho} \right| \Omega \right\rangle = -\frac{1}{4}\sum_j d_{g_j} \left\langle \Omega \left| \frac{\partial \hat{\mathcal{L}}}{\partial g_j} \right| \Omega \right\rangle g_j \ ,$$

where d_{g_j} is the mass dimension of the couplings g_j in the Lagrangian.

The Standard Model of particle physics is a theory that successfully describes all known subatomic particles and the electromagnetic, weak and strong interactions. In this theory we can find two types of terms with a dimensionful coupling: the $\mu^2\phi^\dagger\phi$ term in the Higgs potential and terms that arise from spontaneous symmetry breaking. Spontaneous symmetry breaking means that there is a symmetry of the action that is not realized in the vacuum [3]. In this case it is the Higgs field that has a classical value which is non-zero. This classical value serves as a new, non-trivial ground state of the theory. We can write this as $\sigma \to H + v$, where σ is the scalar field before symmetry breaking and the dimensionful parameter $v \equiv \langle \Omega | \sigma | \Omega \rangle$ indicates the location of the minimum of the potential after symmetry breaking. The terms that follow from symmetry breaking can be linked to the Higgs boson tadpole correction:

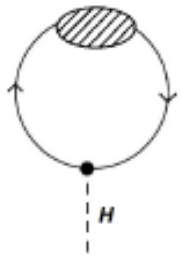

The tadpole correction reflects that quantum corrections shift the position of the minimum of the Higgs potential. We can compensate this by redefining v in terms of the observable minimum v_R and the shift δv. Writing $v = v_R + \delta v$ results in linear terms in the Higgs field that can be used to cancel the tadpole contributions in the Lagrangian. This is called tadpole renormalization. The tadpole contributions, and thus also the corresponding cosmological constant contributions, vanish after renormalization. The terms that arise from spontaneous symmetry breaking do not contribute to the cosmological constant.

2.3 The Higgs Lagrangian

All we are left with is the $\mu^2\phi^\dagger\phi$ term in the Higgs potential, which can be visualized by the following Feynman diagram:

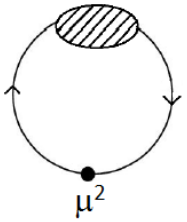

The full Higgs potential is given by $V(\phi) = -\mu^2\phi^\dagger\phi + \lambda(\phi^\dagger\phi)^2$, with $\lambda, \mu^2 > 0$ [5]. The first term is a masslike term, apart from the fact that it has the wrong sign for a usual mass term, and the second term is a 4-point interaction term. The Higgs potential is also called the Mexican hat potential because of its shape:

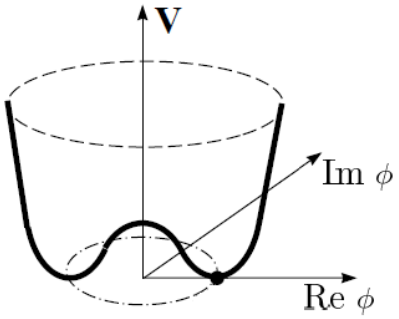

The minima lie in a circle with the non-trivial solution $\phi^\dagger\phi = \frac{\mu^2}{2\lambda} \equiv \frac{v^2}{2}$. We need to choose a minimum and redefine our theory with respect to the new ground state as mentioned before.
We can write the Lagrangian of the Higgs part of the Standard model as:

$$\begin{aligned}\mathcal{L}_H &= T(\phi) - V(\phi) \\ &= (\partial_\mu\phi)^\dagger(\partial^\mu\phi) + \mu^2\phi^\dagger\phi - \lambda(\phi^\dagger\phi)^2 \ .\end{aligned}$$

When expanding the field around the chosen minimum and coupling it to the other fields in the Standard Model we get an interesting result: the interaction strength of the Higgs to other particles is proportional to their masses. In the Standard Model this means that the Higgs couples strongest to the top quark, which has a mass of 173 GeV. The mass of the Higgs boson itself, $m_H^2 = 2\lambda v^2$, is not predicted by the theory, because λ is a free parameter.

Until the discovery of the Higgs boson in 2012 the mass of the Higgs boson was unknown. Only the vacuum expectation v was known. There were upper and lower bounds on the Higgs mass by requiring that the self-coupling λ remained finite and positive at higher energies [3][5]. The coupling namely isn't constant, as we will see in the next subsection, but is dependent on the energy. Even now that the Higgs mass is known, these bounds still have some relevance. The upper bound, also called the triviality bound, is found by assuming that the self-coupling doesn't have a Landau pole. A coupling has a Landau pole if it becomes infinite at some finite energy. This implies that perturbation theory breaks down near the Landau pole and new physics has to kick in. For the

Standard Model to hold up to some cutoff scale Λ_c we require that $\lambda(\Lambda_c) < \infty$ up to that scale. This puts an upper bound on the Higgs self-coupling and therefore on the Higgs mass. For the Planck scale $\Lambda_P = 10^{19}$ GeV the upper limit on the Higgs mass is about 160 GeV. On the other hand we have to worry that the self-coupling doesn't go through zero, since negative vaules of λ would correspond to an unstable Higgs potential. It wouldn't be bounded from below, so no consistent theory could be constructed. Therefore we require that λ remains positive up to the cutoff scale. This leads to a lower bound on the Higgs mass, which is called the stability bound. For the Planck scale we get a lower bound of about 130 GeV. In Figure 1 the theoretically allowed range of Higgs masses is shown as a function of Λ_c.
For the measured Higgs mass $m_H = 125$ GeV we are actually in the meta-stable region according to this calculation, meaning that the universe is in a local minimum of the Higgs potential, but not in the global minimum. There is no need to worry however, because the tunneling time through the potential barrier is larger than the lifetime of the universe.

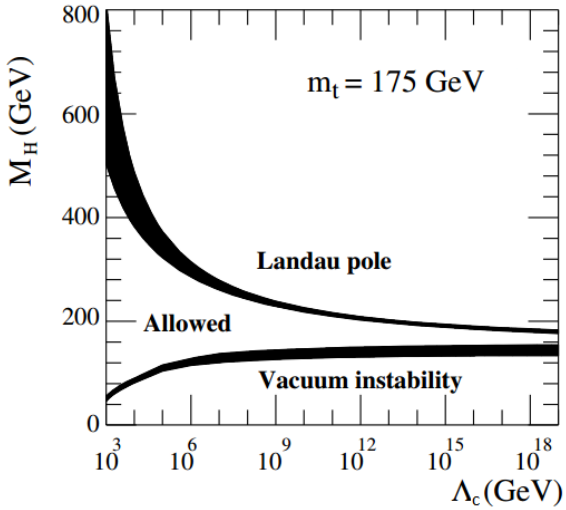

Figure 1: Upper and lower bound on the Higgs mass

2.4 Scalar Yukawa theory

In the calculation of the $\mu^2\phi^\dagger\phi$-term we have to take into account the self-energy of the Higgs field. This self-energy depends on the field theory that is used. Our research is purely about comparing the vacuum bubble to the renormalization group equation. Therefore we will not be looking at the Standard Model Lagrangian, but we will use the scalar Yukawa theory to avoid unnecessarily difficult calculations regarding spin and gauge invariance. The Lagrangian for the scalar Yukawa theory is given by [1]:

$$\mathcal{L} = (\partial_\mu \Psi^*)(\partial^\mu \Psi) + \frac{1}{2}(\partial_\mu \phi)(\partial^\mu \phi) - M^2\Psi^*\Psi - \frac{1}{2}m^2\phi^2 - g\Psi^*\Psi\phi.$$

The first two terms are kinetic terms, the third and fourth are mass terms and the last one is the interaction term. This theory couples a complex scalar field Ψ of mass M to a real scalar field ϕ of mass m. The coupling constant g is a measure of the interaction strength. It is real and has mass dimension 1. Given the Lagrangian we can determine the momentum-space Feynman rules:

- For each ϕ-propagator insert $\frac{i}{p^2-m^2+i\epsilon}$.
- For each Ψ-propagator insert $\frac{i}{p^2-M^2+i\epsilon}$.
- For each vertex insert $-ig$.
- Impose energy-momentum conservation at each vertex.
- Integrate over each undetermined loop momentum l: $\int \frac{d^4l}{(2\pi)^4}$.

These are the Feynman rules we will use to calculate the vacuum diagram in chapter 3.

The scalar Yukawa theory is just a toy model; it is a simplification of the Yukawa theory. The Yukawa theory describes the interaction between scalars and fermions in the Standard Model. Apart from spin aspects the two theories differ in the dimension of the coupling constant, being +1 for the scalar Yukawa theory and 0 for the true Yukawa theory.

2.5 Renormalization

In our research we want to compare the vacuum diagram to the renormalization group equation. Up until now we have looked at the first part. In this last section we will look at the other side of the story: renormalization. Renormalization is used to handle quantum fluctuations in a field theory. These quantum fluctuations arise due to loops of virtual particles. Inside the loops particles of all energies are taken into account, which results in UV divergences. We are actually assuming the theory to be valid up to arbitrarily high energy scales, or equivalently, arbitrarily small length scales, which is not very realistic.

The first step of renormalization is regularization, which is needed to quantify the divergences. There are multiple regularization methods, but since they have no physical meaning they must all lead to the same result. The two methods we will use in our research are cutoff regularization and dimensional regularization. The cutoff method reflects that quantum field theory is an effective field theory with Λ_c marking the threshold beyond which quantum field theory ceases to be valid. After introducing the cutoff the integral is finite, but depends on the cutoff. The drawback of this method is that it doesn't always respect Lorentz invariance, which is an important property of the vacuum. This situation arises for example when integrating over a Lorentz invariant function, while the cutoff transforms under Lorentz transformations. Dimensional regularization does respect Lorentz invariance. The idea behind dimensional regularization is to integrate over loop momenta in $3-\epsilon$ spatial dimensions (with ϵ infinitesimal) instead of in 3 dimensions.

The next step of renormalization is reparametrization. A Lagrangian contains

so-called bare parameters; parameters that are not measurable. We have to reparameterize the theory in terms of physical (measurable) quantities, called renormalized parameters. If the theory is renormalizable all divergences can be absorbed into a finite number of parameters (coupling constants, masses and field normalizations), which turns the singular theory into a well-defined one. The renormalized parameters are defined at some reference energy scale μ. The bare couplings and the cutoff scale are both fixed, so this must mean that the renormalized couplings change when μ changes. The coupling 'constant' is not a constant anymore, but a function of the energy scale. This phenomenon is called the running of the couplings and is described by the so-called renormalization group equations (RGEs) [6]. The dependence on μ can be determined by stating that physical observables should be independent of the arbitrary renormalization scale. For an observable Γ it should hold that:

$$\frac{d\Gamma}{d\mu} = 0 \ .$$

Doing this for several observables leads to a set of coupled differential equations, the RGEs. It is convenient to multiply the RGEs by a constant. We define:

$$\beta(\Gamma) = 16\pi^2 \frac{d\Gamma}{dt} \ ,$$

where $t \equiv \ln(\frac{\mu}{\mu_0})$ and μ_0 is an (arbitrary) energy scale that makes the argument of the logarithm dimensionless. These are called β-functions and describe how parameters depend on the renormalization scale μ. They are usually computed with perturbation theory, so one gets a β-coefficient per order in perturbation theory.

3 Research

In the previous chapter we looked into the theoretical context of our research. We studied the cosmological constant problem and discovered that only one term in the Standard Model Lagrangian contributes to the cosmological constant: the $\mu^2\phi^\dagger\phi$ term in the Higgs potential. It can be visualized by the following Feynman diagram:

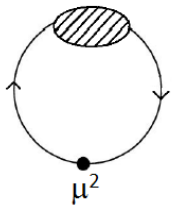

In this chapter we will calculate this diagram up to first order in perturbation theory. We will then compare it to the corresponding renormalization group equation.

3.1 The 1-loop self-energy

The first step is to calculate the 1-loop self-energy $-i\Sigma_2$. Using the Feynman rules for the scalar Yukawa theory we get

$-i\Sigma_2(l^2) \equiv$

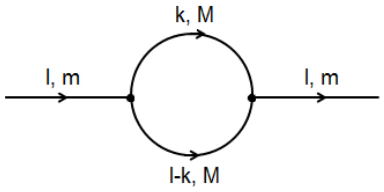

$$= (-ig)^2 \int \frac{d^4k}{(2\pi)^4} \frac{i}{k^2 - M^2 + i\epsilon} \frac{i}{(l-k)^2 - M^2 + i\epsilon} \,. \tag{1}$$

The integrand in this expression has four poles in the complex k^0-plane. We can use a calculational trick called Feynman parametrization to bring this back to two [1]. Feynman parametrization is a well-known technique for evaluating loop integrals. The trick is to combine the two denominators into one using the following equation:

$$\frac{1}{D_1 D_2} = \int_0^1 d\alpha_1 \int_0^1 d\alpha_2 \, \delta(\alpha_1 + \alpha_2 - 1) \frac{1}{(\alpha_1 D_1 + \alpha_2 D_2)^2} \,.$$

The α_n are called Feynman parameters. In our case we have that $D_1 = k^2 - M^2 + i\epsilon$ and $D_2 = (l-k)^2 - M^2 + i\epsilon$. Inserting this into equation (1) leads to

the expression

$$
\begin{aligned}
& g^2 \int_0^1 d\alpha_1 \int_0^1 d\alpha_2 \int \frac{d^4k}{(2\pi)^4}\, \delta(\alpha_1+\alpha_2-1) \\
& \cdot \frac{1}{(\alpha_1(k^2-M^2+i\epsilon)+\alpha_2((l-k)^2-M^2+i\epsilon))^2} \\
&= g^2 \int_0^1 d\alpha_2 \int \frac{d^4k}{(2\pi)^4} \frac{1}{(k^2-M^2+\alpha_2 l^2-2\alpha_2 l\cdot k+i\epsilon)^2} \\
&= g^2 \int_0^1 d\alpha_2 \int \frac{d^4q}{(2\pi)^4} \frac{1}{(q^2-\Delta+i\epsilon)^2}\ . \qquad (2)
\end{aligned}
$$

In the last step we changed the integration variable from k to $q \equiv k - \alpha_2 l$ and defined the parameter $\Delta \equiv M^2 - \alpha_2(1-\alpha_2)l^2$.
We can now perform a Wick rotation to transform the Minkowskian integral into a Euclidean one [1]. To that end we use the integration contour C indicated in Figure 2 to perform the q^0-part of the integral. Since the poles are situated outside the integration contour, the integral along the real q^0-axis is transformed into an integral along the imaginary axis:

$$
\int_{-\infty}^{\infty} dq^0 \rightarrow -\int_{i\infty}^{-i\infty} dq^0 \overset{q^0 \equiv i q_E^0}{=\!=\!=} -i \int_{\infty}^{-\infty} dq_E^0 = i \int_{-\infty}^{\infty} dq_E^0 \quad \text{and} \quad \int d\vec{q} \overset{\vec{q}\equiv\vec{q}_E}{=\!=\!=} \int d\vec{q}_E\ ,
$$

where we use the subscript E to indicate that we are working in Euclidean space.

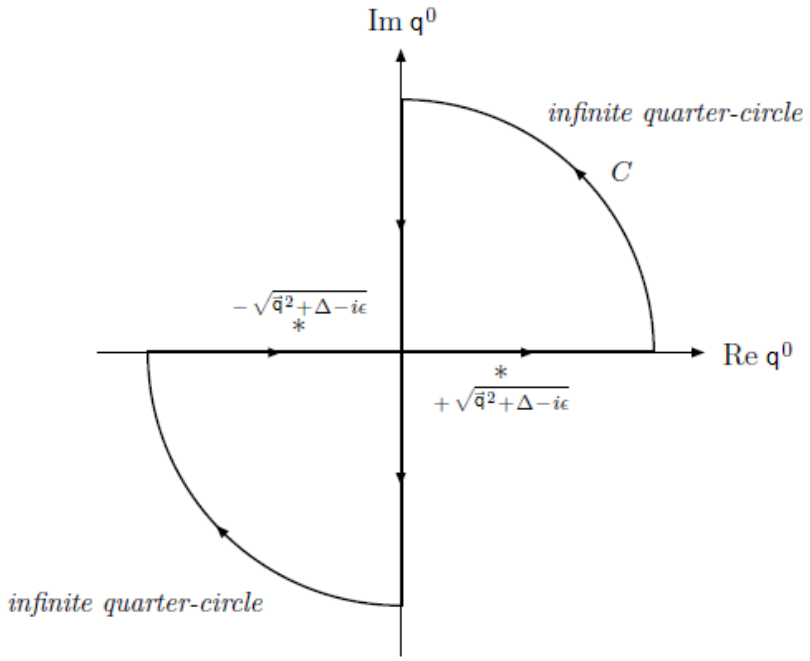

Figure 2: Closed integration contour used for performing Wick rotation

Inserting this into equation (2) leads to

$$\begin{aligned}
& ig^2 \int_0^1 d\alpha_2 \int \frac{dq_E^0}{2\pi} \int \frac{d\vec{q}_E}{(2\pi)^3} \frac{1}{[-(q_E^0)^2 - \vec{q}_E^2 - \Delta + i\epsilon]^2} \\
&= \frac{ig^2}{16\pi^4} \int_0^1 d\alpha_2 \int \frac{d^4 q_E}{(q_E^2 + \Delta - i\epsilon)^2} \\
&= \frac{ig^2}{16\pi^4} \int_0^1 d\alpha_2 \int_0^{2\pi} d\theta_1 \int_0^{\pi} d\theta_2 \sin(\theta_2) \int_0^{\pi} d\theta_3 \sin^2(\theta_3) \\
&\quad \cdot \frac{1}{2} \int_0^{\infty} dq_E^2 \, \frac{q_E^2}{(q_E^2 + \Delta - i\epsilon)^2} \\
&= \frac{ig^2}{16\pi^2} \int_0^1 d\alpha_2 \int_0^{\infty} dq_E^2 \, \frac{q_E^2}{(q_E^2 + \Delta - i\epsilon)^2} \, . \qquad (3)
\end{aligned}$$

In the third line we used that in an n-dimensional Euclidean space the transition to spherical coordinates is given by:

$$\begin{aligned}
\int d\vec{r} \, f(r) &= \int_0^{\infty} dr \; r^{n-1} f(r) \int_0^{2\pi} d\theta_1 \int_0^{\pi} d\theta_2 \sin\theta_2 ... \int_0^{\pi} d\theta_{n-1} \sin^{n-2}\theta_{n-1} \\
&= \frac{2\pi^{n/2}}{\Gamma(n/2)} \int_0^{\infty} dr \; r^{n-1} f(r) \, ,
\end{aligned}$$

where the gamma function $\Gamma(z)$ satisfies $\Gamma(1/2) = \sqrt{\pi}, \Gamma(1) = 1$ and $\Gamma(z+1) = z\Gamma(z)$.
In equation (3) we see a UV divergence emerging from the large-momentum regime $q_E^2 \to \infty$. To quantify the UV divergence we introduce an energy cutoff scale Λ_c and assume $\Lambda_c^2 >> \Delta$:

$$\begin{aligned}
& \frac{ig^2}{16\pi^2} \int_0^1 d\alpha_2 \int_0^{\Lambda_c^2} dq_E^2 \, \frac{q_E^2}{(q_E^2 + \Delta - i\epsilon)^2} \\
&= \frac{ig^2}{16\pi^2} \int_0^1 d\alpha_2 \left[\log(q_E^2 + \Delta - i\epsilon) + \frac{\Delta - i\epsilon}{q_E^2 + \Delta - i\epsilon} \right]_{q_E^2 = 0}^{q_E^2 = \Lambda_c^2} \\
&= \frac{ig^2}{16\pi^2} \int_0^1 d\alpha_2 [\log(\Lambda_c^2) - \log(\Delta - i\epsilon) - 1] \\
&= \frac{ig^2}{16\pi^2} \left([\alpha_2 \log(\Lambda_c^2)]_0^1 - [\alpha_2]_0^1 - \int_0^1 d\alpha_2 \log(\Delta - i\epsilon) \right) \\
&= \frac{ig^2}{16\pi^2} \left(\log(\Lambda_c^2) - 1 - \int_0^1 d\alpha_2 \log(M^2 + \alpha_2^2 l^2 - \alpha_2 l^2 - i\epsilon) \right) \, . \qquad (4)
\end{aligned}$$

The logarithm in equation (4) gives rise to a branch cut for $M^2 + \alpha_2^2 \, l^2 - \alpha_2 l^2 \in \mathbb{R}^-$, since $\log(-x \pm i\epsilon) = \log(xe^{\pm i\pi}) = \log(x) \pm i\pi$ for $x > 0$. To solve the integral we need to factorize the expression in the logarithm. This factorization depends on the domain we are in, because we have to make sure the factors can't become negative. Therefore we will solve the integral in three domains: $l^2 < 0$, $0 < l^2 < 4M^2$ and $l^2 > 4M^2$. To improve the readability we rename α_2 to x.

Domain 1: $l^2 < 0$:
In the domain $l^2 < 0$ we can factorize the expression in the logarithm by using $x_\pm = \frac{1}{2}(1 \pm \beta_1)$ with $\beta_1 = \sqrt{1 - \frac{4M^2 - 4i\epsilon}{l^2}}$. This means that $\beta_1 > 1$, $l^2 = \frac{4M^2 - 4i\epsilon}{1-\beta_1^2}$ and $1 - x_+ = x_-$. Then we can calculate the integral:

$$\begin{aligned}
&\int_0^1 dx\ \log\left(M^2 + x^2 l^2 - x l^2 - i\epsilon\right) \\
=&\int_0^1 dx\ \left[\log\left(-l^2\right) + \log(x_+ - x) + \log(x - x_-)\right] \\
=&-2 + \log\left(-l^2\right) + (1 - x_+)\log\left(x_+ - 1\right) + (1 - x_-)\log\left(1 - x_-\right) \\
&+ x_+ \log\left(x_+\right) + x_- \log\left(-x_-\right) \\
=&-2 + \log\left(-l^2 x_-^2\right) + 2x_+[\log\left(x_+\right) - \log\left(-x_-\right)] \\
=&-2 + \log\left(M^2 \cdot \frac{\beta_1 - 1}{\beta_1 + 1}\right) + (1 + \beta_1)\log\left(\frac{\beta_1 + 1}{\beta_1 - 1}\right) \\
=&-2 + \log\left(M^2\right) + \beta_1 \log\left(\frac{\beta_1 + 1}{\beta_1 - 1}\right).
\end{aligned}$$

Domain 2: $0 < l^2 < 4M^2$:
In the domain $0 < l^2 < 4M^2$ we use $x_\pm = \frac{1}{2}(1 \pm i\beta_2)$ with $\beta_2 = \sqrt{\frac{4M^2 - 4i\epsilon}{l^2} - 1}$. This way $\beta_2 > 0$, $l^2 = \frac{4M^2 - 4i\epsilon}{\beta_2^2 + 1}$ and $1 - x_+ = x_-$. Then we get:

$$\begin{aligned}
&\int_0^1 dx\ \log\left(M^2 + x^2 l^2 - x l^2 - i\epsilon\right) \\
=&\int_0^1 dx\ \left[\log\left(l^2\right) + \log(x - x_+) + \log(x - x_-)\right] \\
=&-2 + \log\left(l^2\right) + (1 - x_+)\log\left(1 - x_+\right) + (1 - x_-)\log\left(1 - x_-\right) \\
&+ x_+ \log\left(-x_+\right) + x_- \log\left(-x_-\right) \\
=&-2 + \log\left(-l^2 x_-^2\right) + x_+[-\log\left(x_-\right) + \log\left(x_+\right) + \log\left(-x_+\right) - \log\left(-x_-\right)] \\
=&-2 + \log\left(M^2 \cdot \frac{i\beta_2 - 1}{i\beta_2 + 1}\right) + (1 + i\beta_2)\log\left(\frac{i\beta_2 + 1}{i\beta_2 - 1}\right) \\
=&-2 + \log\left(M^2\right) + i\beta_2 \log\left(\frac{i\beta_2 + 1}{i\beta_2 - 1}\right) \\
=&-2 + \log\left(M^2\right) + 2\beta_2 \arctan\left(\frac{1}{\beta_2}\right).
\end{aligned}$$

In the last line we used that $i \log\left(\frac{1 - iz}{1 + iz}\right) = 2 \arctan(z)$.

Domain 3: $l^2 > 4M^2$:
Finally, in the domain $l^2 > 4M^2$ we can factorize the expression by using $x_\pm = \frac{1}{2}(1 \pm \beta_3)$ with $\beta_3 = \sqrt{1 - \frac{4M^2 - 4i\epsilon}{l^2}}$. This results in $0 < \beta_3 < 1$,

$l^2 = \frac{4M^2 - 4i\epsilon}{1-\beta_3^2}$ and $1 - x_+ = x_-$. Then we get for the integral:

$$\begin{aligned}
&\int_0^1 dx\ \log\left(M^2 + x^2 l^2 - x l^2 - i\epsilon\right) \\
&= \int_0^1 dx\ \left[\log\left(l^2\right) + \log(x - x_+) + \log(x - x_-)\right] \\
&= -2 + \log\left(l^2\right) + (1 - x_+)\log\left(1 - x_+\right) + (1 - x_-)\log\left(1 - x_-\right) \\
&\quad + x_+ \log\left(-x_+\right) + x_- \log\left(-x_-\right) \\
&= -2 + \log\left(-l^2 x_-^2\right) + x_+\left[-\log\left(x_-\right) + \log\left(x_+\right) + \log\left(-x_+\right) - \log\left(-x_-\right)\right] \\
&= -2 + \log\left(M^2 \cdot \frac{\beta_3 - 1}{\beta_3 + 1}\right) + (1 + \beta_3)\log\left(\frac{\beta_3 + 1}{\beta_3 - 1}\right) \\
&= -2 + \log\left(M^2\right) + \beta_3 \log\left(\frac{\beta_3 + 1}{\beta_3 - 1}\right).
\end{aligned}$$

Substituting the results per domain into equation (4) leads to:

- $l^2 < 0 : \frac{ig^2}{16\pi^2}\left(1 + \log\left(\frac{\Lambda_c^2}{M^2}\right) - \sqrt{1 - \frac{4M^2}{l^2}}\log\left(\frac{\sqrt{1-\frac{4M^2}{l^2}}+1}{\sqrt{1-\frac{4M^2}{l^2}}-1}\right)\right)$
- $0 < l^2 < 4M^2 : \frac{ig^2}{16\pi^2}\left(1 + \log\left(\frac{\Lambda_c^2}{M^2}\right) - 2\sqrt{\frac{4M^2}{l^2} - 1}\arctan\left(\frac{1}{\sqrt{\frac{4M^2}{l^2}-1}}\right)\right)$
- $l^2 > 4M^2 : \frac{ig^2}{16\pi^2}\left(1 + \log\left(\frac{\Lambda_c^2}{M^2}\right) - \sqrt{1 - \frac{4M^2}{l^2}}\left[\log\left(\frac{\sqrt{1-\frac{4M^2}{l^2}}+1}{\sqrt{1-\frac{4M^2}{l^2}}-1}\right) - i\pi\right]\right)$

In the first and second domain we can just leave out the $-i\epsilon$ term, because there are no poles in these domains. In the third domain however we cross the branch cut, which gives rise to the $-i\pi$ term.
We now have the result for the 1-loop self-energy per momentum domain. In order to calculate the vacuum bubble contribution we need one result for all domains. A method called analytic continuation offers a way of extending a function throughout the entire complex plane, except where the function is singular. According to this method the three formulas can be summarized by [7]:

$$\frac{ig^2}{16\pi^2}\left(1 + \log\left(\frac{\Lambda_c^2}{M^2}\right) - x_+ \log\left(\frac{x_+}{x_+ - 1}\right) - x_- \log\left(\frac{x_-}{x_- - 1}\right)\right),$$

with $x_\pm = \frac{1}{2}\left(1 \pm \sqrt{1 - \frac{4M^2}{l^2 + i\epsilon}}\right)$.

In our case this leads to the result

$$-i\Sigma_2(l^2) \equiv$$

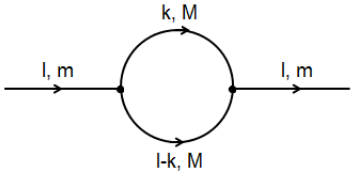

$$= \frac{ig^2}{16\pi^2}\left(1 + \log\left(\frac{\Lambda_c^2}{M^2}\right) - \sqrt{1 - \frac{4M^2}{l^2 + i\epsilon}}\right.$$
$$\left. \cdot \log\left(\frac{\sqrt{1 - \frac{4M^2}{l^2+i\epsilon}} + 1}{\sqrt{1 - \frac{4M^2}{l^2+i\epsilon}} - 1}\right)\right) . \qquad (5)$$

3.2 The Källén-Lehmann spectral representation

Now that we have the final result for the 1-loop self-energy, we can take the next step in our calculation. Up to first order in perturbation theory the dressed Higgs propagator is given by a Dyson summation:

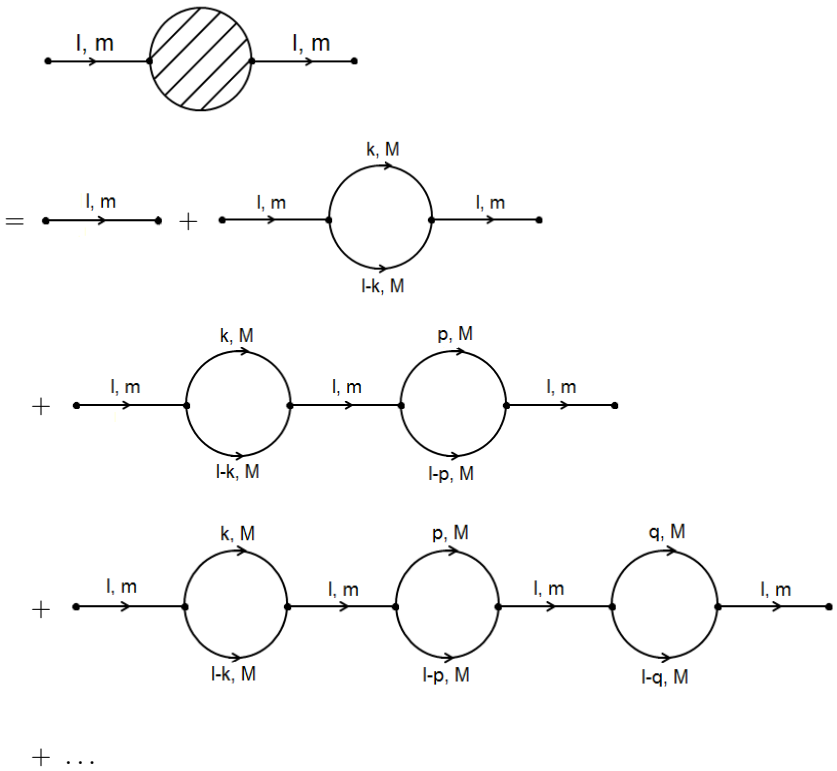

$+ \ldots$

$$
\begin{aligned}
&= \frac{i}{l^2 - m^2 + i\epsilon} + \frac{i}{l^2 - m^2 + i\epsilon}(-i\Sigma_2(l^2))\frac{i}{l^2 - m^2 + i\epsilon} \\
&\quad + \frac{i}{l^2 - m^2 + i\epsilon}(-i\Sigma_2(l^2))\frac{i}{l^2 - m^2 + i\epsilon}(-i\Sigma_2(l^2))\frac{i}{l^2 - m^2 + i\epsilon} \\
&\quad + \frac{i}{l^2 - m^2 + i\epsilon}(-i\Sigma_2(l^2))\frac{i}{l^2 - m^2 + i\epsilon}(-i\Sigma_2(l^2))\frac{i}{l^2 - m^2 + i\epsilon} \\
&\quad (-i\Sigma_2(l^2))\frac{i}{l^2 - m^2 + i\epsilon} + ... \\
&= \frac{i}{l^2 - m^2 - \Sigma_2(l^2) + i\epsilon}\,, \qquad (6)
\end{aligned}
$$

with $\Sigma_2(l^2)$ defined by equation (5). The next step would be to perform the loop integral over momentum l. With the function $\Sigma_2(l^2)$ in the denominator this would be a very hard task though. We will therefore use the Källén-Lehmann spectral representation. For the 2-point Green's function it is given by:

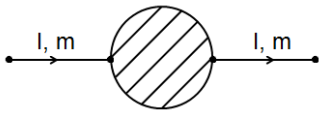

$$= \frac{1}{2\pi}\int_0^\infty dq^2\ \frac{i\rho(q^2)}{l^2 - q^2 + i\epsilon}\,. \qquad (7)$$

The function $\rho(q^2)$ can be seen as a spectral density function. It captures the pole- and cutstructure of the diagram and needs to be related to the 1-loop self-energy we calculated. We can deduce the relationship between $\rho(q^2)$ and $\Sigma_2(q^2)$ from Cauchy's integral formula [8]. This formula tells us that a holomorphic function defined on a disk is completely determined by its values on the boundary of the disk. It can be said that for every a in the interior of a closed contour γ that

$$f(a) = \frac{1}{2\pi i}\oint_\gamma dz\ \frac{f(z)}{z - a}\,.$$

We can use this formula for our function $f(l^2) \equiv \frac{1}{l^2 - m^2 - \Sigma_2(l^2) + i\epsilon}$. This function has a pole at the physical mass m_p of the particle and a branch-cut from $4M^2$ onwards. Let γ be the contour indicated in Figure 3. We can assume the function $f(l^2)/l^2$ to go to zero fast enough on the infinite circular part of the contour. Then Cauchy's integral formula tells us that for every l^2 in the interior of γ:

$$
\begin{aligned}
f(l^2) &= \frac{1}{2\pi i}\oint_\gamma dq^2 \frac{f(q^2)}{q^2 - l^2} \\
&= \frac{1}{2\pi i}\int_0^\infty dq^2\ \frac{Disc(f(q^2))}{q^2 - l^2} \\
&= \frac{1}{\pi}\int_0^\infty dq^2\ \frac{Im(f(q^2))}{q^2 - l^2}\,. \qquad (8)
\end{aligned}
$$

In the third line we used that the discontinuity equals $2i$ times the imaginary part. Equation (8) is called a dispersion relation.

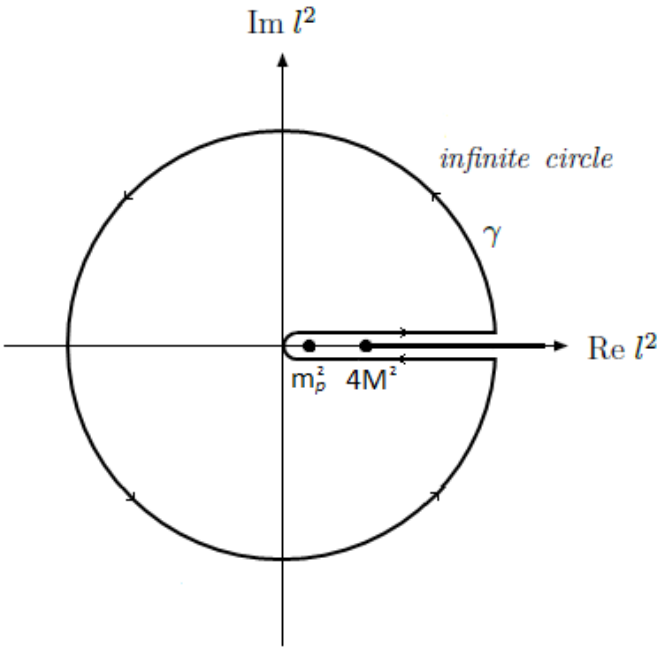

Figure 3: Cauchy integral contour

By comparing equation (8) to equation (7) we can extract the spectral density function:

$$\begin{aligned}\rho(q^2) &= -2\, Im(f(q^2)) \\ &= -2\, Im\left(\frac{1}{q^2 - m^2 - \Sigma_2(q^2) + i\epsilon}\right) \ . \end{aligned} \tag{9}$$

To get an idea of where the imaginary parts come from and what structure the spectral density function will have, it is easiest to approach it from a diagrammatic point of view. The imaginary part of an individual propagator originates from the $i\epsilon$ part:

$$\frac{1}{l^2 - m^2 + i\epsilon} = \frac{l^2 - m^2}{(l^2 - m^2)^2 + \epsilon^2} - \frac{i\epsilon}{(l^2 - m^2)^2 + \epsilon^2} = P\left(\frac{1}{l^2 - m^2}\right) - i\pi\delta(l^2 - m^2) \ ,$$

where P stands for the principal value. Discontinuities thus come from intermediate particles becoming on-shell.
The discontinuity of a Feynman diagram can then be obtained using the so-called Cutkosky cutting rules:

- Cut the diagram in all possible ways, with all cut propagators becoming on-shell simultaneously.
- Replace $\frac{i}{l^2 - m^2 + i\epsilon}$ by $2\pi\theta(l_0)\delta(l^2 - m^2)$ in each cut propagator.
- Use the complex conjugate at the right hand side of the cut.
- Sum contributions of all possible cuts.

We can use these rules to determine the discontinuities of the diagrams in our Dyson summation in equation (6). First of all, the propagator becomes:

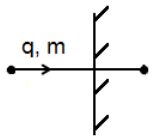

$$= 2\pi\delta(q^2 - m^2)\ , \tag{10}$$

which originates from the one-particle pole.
For the Feynman diagram with one loop we have:

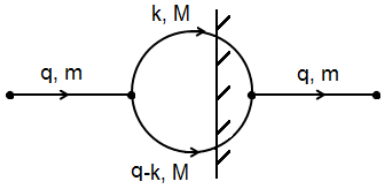

$$\begin{aligned}
&= \frac{i}{q^2 - m^2 + i\epsilon}(-ig)\int \frac{d^4k}{(2\pi)^4}\, 2\pi\theta(k_0)\delta(k^2 - M^2)2\pi\theta(q_0 - k_0) \\
&\quad \delta((q-k)^2 - M^2)(ig)\frac{-i}{q^2 - m^2 - i\epsilon} \\
&= \frac{g^2}{4\pi^2}\frac{1}{(q^2 - m^2)^2}\int d^4k\ \theta(k_0)\delta(k^2 - M^2)\theta(q_0 - k_0)\delta((q-k)^2 - M^2)
\end{aligned}$$

We can now choose to go to the rest frame such that $\vec{q} = \vec{0}$, $q_0 = \sqrt{q^2}$ and $(q-k)^2 = q^2 + k^2 - 2k_0\sqrt{q^2}$. We write $\int d^4k = \int dk_0 \int d\vec{k}$, use spherical coordinates and introduce the new variable $w = \sqrt{\vec{k}^2 + M^2}$. Then we get:

$$\begin{aligned}
&= \frac{g^2}{4\pi^2}\frac{1}{(q^2 - m^2)^2}\int dk_0 \int d\vec{k}\ \delta(k^2 - M^2) \\
&\quad \cdot \delta(q^2 + k^2 - 2k_0\sqrt{q^2} - M^2)\ \theta(k_0)\ \theta(\sqrt{q^2} - k_0) \\
&= \frac{g^2}{\pi}\frac{1}{(q^2 - m^2)^2}\int dk_0 \int_0^\infty d|\vec{k}|\ \vec{k}^{\,2}\ \delta(k^2 - M^2) \\
&\quad \cdot \delta(q^2 + k^2 - 2k_0\sqrt{q^2} - M^2)\ \theta(k_0)\ \theta(\sqrt{q^2} - k_0) \\
&= \frac{g^2}{\pi}\frac{1}{(q^2 - m^2)^2}\int dk_0 \int_M^\infty dw\ w\sqrt{w^2 - M^2}\ \delta(k_0^2 - w^2) \\
&\quad \cdot \delta(q^2 + k_0^2 - 2k_0\sqrt{q^2} - w^2)\ \theta(k_0)\ \theta(\sqrt{q^2} - k_0) \\
&= \frac{g^2}{\pi}\frac{1}{(q^2 - m^2)^2}\int_M^\infty dw\ \frac{1}{2}\sqrt{w^2 - M^2}\ \delta(q^2 - 2w\sqrt{q^2})\ \theta(\sqrt{q^2} - w) \\
&= \frac{g^2}{8\pi}\frac{1}{(q^2 - m^2)^2}\ \theta(q^2 - 4M^2)\sqrt{1 - \frac{4M^2}{q^2}}\ .
\end{aligned} \tag{11}$$

First we solved the k_0 integral, which implied $k_0 = w$. Then we solved the w integral, which led to the conclusion that $w = \sqrt{q^2}/2$.
Equation (11) contributes only for $q^2 \geq 4M^2$. This corresponds to the physical threshold for the process describing the decay into the two intermediate state

particles with mass M. We could continu calculating the discontinuities of the diagrams with more loops, but these will lead to the same structure multiplied by the self-energy $-i\Sigma_2(q^2)$ for loops that are not cut. By summing all diagrams the self-energy will again appear in the denominator.

To get the exact result for the spectral density function it is easier to use equation (9). Let's analyze the formula:

$$\begin{aligned} & Im\left(\frac{1}{q^2-m^2-\Sigma_2(q^2)+i\epsilon}\right) \\ =& \frac{Im\left(q^2-m^2-\Sigma_2^*(q^2)-i\epsilon\right)}{\left|q^2-m^2-\Sigma_2(q^2)+i\epsilon\right|^2} \\ =& \frac{-Im\left(\Sigma_2^*(q^2)\right)-\epsilon}{\left(q^2-m^2-Re\left(\Sigma_2(q^2)\right)\right)^2+\left(\epsilon-Im\left(\Sigma_2(q^2)\right)\right)^2} \ . \end{aligned}$$

For $q^2 < 4M^2$, i.e. preceding the branch-cut, the function $\Sigma_2(q^2)$ doesn't have an imaginary part. Therefore we can say:

$$\begin{aligned} & Im\left(\frac{1}{q^2-m^2-\Sigma_2(q^2)+i\epsilon}\right) \\ =& \frac{-\epsilon}{\left(q^2-m^2-Re(\Sigma_2(q^2))\right)^2+\epsilon^2} \\ \overset{\epsilon\to 0}{=}& \frac{-\pi}{1-Re\left(\Sigma_2'(m_p^2)\right)}\,\delta(q^2-m_p^2) \\ =& -\pi Z\delta(q^2-m_p^2)\ , \end{aligned} \tag{12}$$

with $Z=\frac{1}{1-Re\left(\Sigma_2'(m_p^2)\right)}$ called the field-strength renormalization and m_p being the root of $q^2-m^2-Re(\Sigma_2(q^2))=0$.
For $q^2 \geq 4M^2$, i.e. at the branch-cut, the function $\Sigma_2(q^2)$ does have an imaginary part. We can then write:

$$\begin{aligned} & Im\left(\frac{1}{q^2-m^2-\Sigma_2(q^2)+i\epsilon}\right) \\ =& \frac{-Im(\Sigma_2^*(q^2))}{|q^2-m^2-\Sigma_2(q^2)|^2} \\ =& -\frac{g^2}{16\pi}\,\frac{\sqrt{1-\frac{4M^2}{q^2}}}{|q^2-m^2-\Sigma_2(q^2)|^2}\,\theta(q^2-4M^2)\ . \end{aligned} \tag{13}$$

Now that we know the imaginary part of our diagram, we can determine the spectral density function according to equation (9):

$$\begin{aligned} \rho(q^2) &= -2\,Im\left(\frac{1}{q^2-m^2-\Sigma_2(q^2)+i\epsilon}\right) \\ &= 2\pi Z\delta(q^2-m_p^2)+\frac{g^2}{8\pi}\,\frac{\sqrt{1-\frac{4M^2}{q^2}}}{|q^2-m^2-\Sigma_2(q^2)|^2}\,\theta(q^2-4M^2)\ . \end{aligned} \tag{14}$$

In equation (14) we again recognize contributions from the one-particle pole and the branch-cut. It meets our expectations based on the analysis of the diagrams.

Inserting the spectral density function into equation (7) we find the result for the Källén-Lehmann spectral representation:

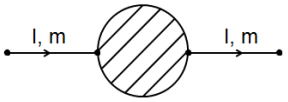

$$
\begin{aligned}
&= \frac{1}{2\pi}\int_0^\infty dq^2\ \frac{i\rho(q^2)}{l^2-q^2+i\epsilon} \\
&= \frac{1}{2\pi}\int_0^\infty dq^2\Bigg[\frac{i}{l^2-q^2+i\epsilon}\cdot 2\pi Z\delta(q^2-m_p^2) \\
&\quad + \frac{g^2}{8\pi}\theta(q^2-4M^2)\frac{\sqrt{1-\frac{4M^2}{q^2}}}{|q^2-m^2-\Sigma_2(q^2)|^2}\frac{i}{l^2-q^2+i\epsilon}\Bigg] \\
&= \frac{iZ}{l^2-m_p^2+i\epsilon} + \frac{g^2}{16\pi^2}\int_{4M^2}^\infty dq^2\sqrt{1-\frac{4M^2}{q^2}} \\
&\quad \cdot \frac{1}{|q^2-m^2-\Sigma_2(q^2)|^2}\frac{i}{l^2-q^2+i\epsilon}\ .
\end{aligned}
$$

3.3 The vacuum bubble

The final step in our calculation is to close the loop by integrating over the loop-momentum l and multiplying by the coupling constant μ^2:

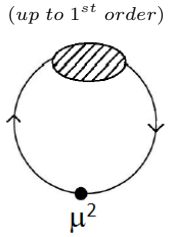

$$
\begin{aligned}
&= \mu^2\int\frac{d^4l}{(2\pi)^4}\Bigg[\frac{iZ}{l^2-m_p^2+i\epsilon} + \frac{g^2}{16\pi^2}\int_{4M^2}^\infty dq^2\sqrt{1-\frac{4M^2}{q^2}} \\
&\quad \cdot \frac{1}{|q^2-m^2-\Sigma_2(q^2)|^2}\frac{i}{l^2-q^2+i\epsilon}\Bigg]\ .
\end{aligned}
$$

It is easiest to solve the integral over the four-momentum l first. Interchanging the q^2 and l integrals is allowed, because the integrand is convergent enough. The l_0-part of the integral can then be solved using the residue theorem as follows:

$$
\begin{aligned}
&\mu^2\int\frac{d\vec{l}}{(2\pi)^3}\Bigg[\int\frac{dl_0}{2\pi}\frac{iZ}{l^2-m_p^2+i\epsilon} + \frac{g^2}{16\pi^2}\int_{4M^2}^\infty dq^2\sqrt{1-\frac{4M^2}{q^2}} \\
&\cdot\frac{1}{|q^2-m^2-\Sigma_2(q^2)|^2}\int\frac{dl_0}{2\pi}\frac{i}{l^2-q^2+i\epsilon}\Bigg] \\
&= \mu^2\int\frac{d\vec{l}}{(2\pi)^3}\Bigg[\frac{Z}{2\sqrt{\vec{l}^2+m_p^2}} + \frac{g^2}{32\pi^2}\int_{4M^2}^\infty dq^2\sqrt{1-\frac{4M^2}{q^2}} \\
&\cdot\frac{1}{|q^2-m^2-\Sigma_2(q^2)|^2}\frac{1}{\sqrt{\vec{l}^2+q^2}}\Bigg]\ .
\end{aligned}
\tag{15}
$$

The function $\Sigma_2(q^2)$ in the denominator of equation (15) leads to a second order correction, whereas we only want to look at our diagram up to first order. Therefore we would like to write $q^2 - m^2 - \Sigma_2(g^2) \approx q^2 - m_p^2$ and neglect the remaining Σ_2-related corrections. The question is whether or not we can set these remaining terms to zero without introducing a pole. If the particle is stable it means that the one-particle pole precedes the branch-cut. This is depicted in Figure (4). In this case $q^2 - m_p^2$ can never be zero for $q^2 \geq 4M^2$ and we can thus set the remainder to zero.

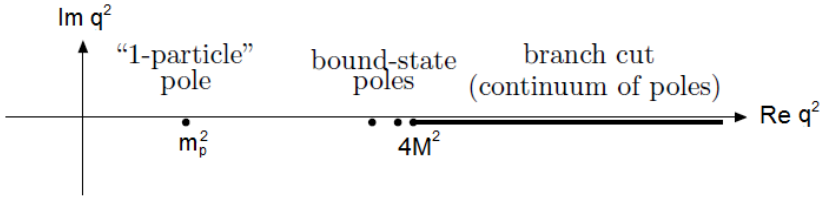

Figure 4: Poles and cuts of the 2-point Green's function for a stable particle

However, for an unstable particle the one-particle pole lies beneath the branch-cut. This is shown in Figure (5). As the pole moves towards the branch-cut it goes below the cut because of the imaginary part of $\Sigma_2(q^2)$. Now $q^2 - m_p^2$ can become zero in the region $q^2 \geq 4M^2$ if we would set the remainder to zero and we would introduce a pole.

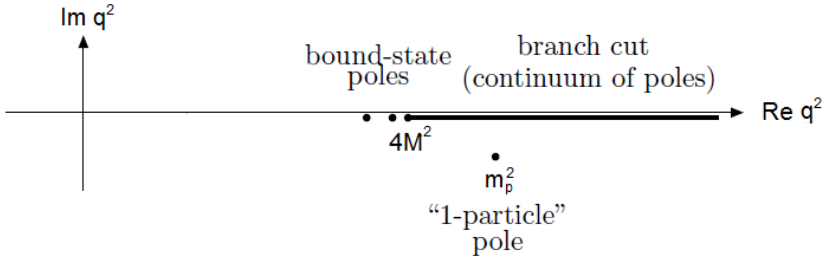

Figure 5: Poles and cuts of the 2-point Green's function for an unstable particle

For now we will assume that the particle is stable, such that we can use the approximation $\Sigma_2(q^2)$=0. Equation (15) then simplifies to:

$$\frac{\mu^2}{2}\int \frac{d\vec{l}}{(2\pi)^3}\frac{Z}{\sqrt{\vec{l}^2+m_p^2}} + \frac{g^2\mu^2}{32\pi^2}\int_{4M^2}^{\infty} dq^2 \sqrt{1-\frac{4M^2}{q^2}}$$
$$\cdot \frac{1}{\left[q^2-m_p^2\right]^2}\int \frac{d\vec{l}}{(2\pi)^3}\frac{1}{\sqrt{\vec{l}^2+q^2}} \cdot$$

To calculate the $\vec{l}$ integral we apply dimensional regularization. Before going into the calculation, we need to define some functions and parameters. First of

all, we make use of the gamma function $\Gamma(t)$ that is defined as

$$\Gamma(t) \equiv \int_0^\infty x^{t-1} e^{-x} dx$$

and satisfies the relation $\Gamma(t+1) = t\Gamma(t)$. In addition we use the beta function $B(x,y) = \Gamma(x)\Gamma(y)/\Gamma(x+y)$:

$$B(x,y) \equiv \int_0^1 t^{x-1}(1-t)^{y-1} dt \ .$$

We assume that in d-dimensional spacetime the momentum still has one temporal component and $d-1$ spatial components. The general expression for the angular integral in $d-1$ dimensions then becomes:

$$\int d\Omega_{d-1} = \frac{2(\pi)^{\frac{d-1}{2}}}{\Gamma(\frac{d-1}{2})} \ .$$

Finally, a scale ν is defined to make sure that the equations are dimensionally correct. Using dimensional regularization, the $\vec{l}$ integral becomes:

$$\begin{aligned}
&\int \frac{d\vec{l}}{(2\pi)^3} \frac{1}{\sqrt{\vec{l}^2 + \Delta^2}} \\
&\to \frac{\nu^{4-d}}{(2\pi)^{d-1}} \int d\Omega_{d-1} \int_0^\infty d|\vec{l}| \frac{|\vec{l}|^{d-2}}{\sqrt{|\vec{l}|^2 + \Delta^2}} \\
&= \frac{\nu^{4-d}}{(2\pi)^{d-1}} \frac{2\pi^{\frac{d-1}{2}}}{\Gamma(\frac{d-1}{2})} \int_0^\infty d|\vec{l}| \frac{|\vec{l}|^{d-2}}{\sqrt{|\vec{l}|^2 + \Delta^2}} \\
&= \frac{\nu^{4-d}}{(2\pi)^{d-1}} \frac{2\pi^{\frac{d-1}{2}}}{\Gamma(\frac{d-1}{2})} \frac{1}{2} \int_0^\infty d\vec{l}^2 \frac{(\vec{l}^2)^{\frac{d-3}{2}}}{\sqrt{\vec{l}^2 + \Delta^2}} \\
&= \frac{\nu^{4-d}}{(4\pi)^{\frac{d-1}{2}}\Gamma(\frac{d-1}{2})} \Delta^{d-2} \int_0^1 dx \, x^{-d/2}(1-x)^{\frac{d-3}{2}} \ .
\end{aligned}$$

In the last step we changed our integration variable from $\vec{l}^2$ to $x = \frac{\Delta^2}{\vec{l}^2 + \Delta^2}$. We now recognize the beta function $B(1-\frac{d}{2}, \frac{d-1}{2}) = \Gamma(1-\frac{d}{2})\Gamma(\frac{d-1}{2})/\Gamma(\frac{1}{2})$. Inserting this leads to:

$$\begin{aligned}
&\frac{\nu^{4-d}}{(4\pi)^{\frac{d-1}{2}}\Gamma(\frac{d-1}{2})} \Delta^{d-2} \int_0^1 dx \, x^{-d/2}(1-x)^{\frac{d-3}{2}} \\
&= \frac{\nu^{4-d}}{(4\pi)^{\frac{d-1}{2}}\Gamma(\frac{d-1}{2})} \Delta^{d-2} \frac{\Gamma(1-\frac{d}{2})\Gamma(\frac{d-1}{2})}{\Gamma(\frac{1}{2})} \\
&= \frac{1}{\sqrt{\pi}} \nu^{4-d} (4\pi)^{\frac{1-d}{2}} \Delta^{d-2} \Gamma\left(1-\frac{d}{2}\right) \\
&= \frac{1}{\sqrt{\pi}} \frac{\nu^4}{\Delta^2} (4\pi)^{\frac{1-d}{2}} \left(\frac{\Delta}{\nu}\right)^d \Gamma\left(1-\frac{d}{2}\right) \ . \qquad (16)
\end{aligned}$$

In our case we are interested in the behavior of equation (16) for d $\to 4$. Thereto we calculate it for $d = 4 - \epsilon$, where in the end we perform a Taylor expansion around $\epsilon = 0$. In order to do this we need the derivative of the gamma function $\Gamma'(t) \equiv d\Gamma(t)/dt$, which is related to the digamma function $\Psi(t) = \Gamma'(t)/\Gamma(t)$. Furthermore it can be used that $\Gamma(1) = 1$ and $\Psi(1) = -\gamma$, with $\gamma \approx 0.577$ called the Euler-Mascheroni constant. Now we can evaluate the Taylor expansions needed to work out equation (16):

$$\begin{aligned}
\Gamma\left(1 - \frac{d}{2}\right) &= \Gamma\left(-1 + \frac{\epsilon}{2}\right) \\
&= \frac{1}{-1 + \frac{\epsilon}{2}} \, \frac{2}{\epsilon} \, \Gamma\left(1 + \frac{\epsilon}{2}\right) \\
&\approx \left(-\frac{2}{\epsilon} - 1\right) \left(\Gamma(1) + \frac{\epsilon}{2}\Psi(1)\Gamma(1)\right) \\
&= \left(-\frac{2}{\epsilon} - 1\right) \left(1 - \frac{\epsilon\gamma}{2}\right) \, .
\end{aligned}$$

$$\begin{aligned}
\left(\frac{\Delta}{\nu}\right)^d &= \left(\frac{\Delta}{\nu}\right)^{4-\epsilon} \\
&= \left(\frac{\Delta}{\nu}\right)^4 \left(\frac{\Delta}{\nu}\right)^{-\epsilon} \\
&\approx \left(\frac{\Delta}{\nu}\right)^4 \left(1 - \epsilon \ln\left(\frac{\Delta}{\nu}\right)\right) \, .
\end{aligned}$$

$$\begin{aligned}
(4\pi)^{\frac{1-d}{2}} &= (4\pi)^{-3/2+\epsilon/2} \\
&= (4\pi)^{-3/2}(4\pi)^{\epsilon/2} \\
&\approx \frac{1}{(4\pi)^{3/2}} \left(1 + \frac{\epsilon}{2} \ln(4\pi)\right) \, .
\end{aligned}$$

Our result for the $\vec{l}$ integral then becomes:

$$\begin{aligned}
\int \frac{d\vec{l}}{(2\pi)^3} \frac{1}{\sqrt{\vec{l}^2 + \Delta^2}} &= \frac{1}{\sqrt{\pi}} \frac{\nu^4}{\Delta^2} \frac{1}{(4\pi)^{3/2}} \left(1 + \frac{\epsilon}{2} \ln(4\pi)\right) \left(\frac{\Delta}{\nu}\right)^4 \\
&\quad \cdot \left(1 - \epsilon \ln\left(\frac{\Delta}{\nu}\right)\right) \left(-\frac{2}{\epsilon} - 1\right) \left(1 - \frac{\epsilon\gamma}{2}\right) \\
&= -\frac{\Delta^2}{8\pi^2} \left(\frac{2}{\epsilon} + 1 - \gamma - \ln\left(\frac{\Delta^2}{4\pi\nu^2}\right)\right) + \ldots \, .
\end{aligned}$$

The dots on the last line represent higher order terms in ϵ. To get rid of the pole $1/\epsilon$ we need to renormalize, but we will leave this to follow-up research. For now we will conserve the structure. We then find the final expression for the vacuum bubble:

$(up\ to\ 1^{st}\ order)$

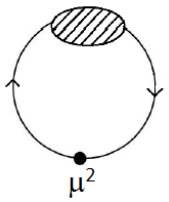

$$
\begin{aligned}
&= \frac{\mu^2}{2}\int \frac{d\vec{l}}{(2\pi)^3}\frac{Z}{\sqrt{\vec{l}^2+m_p^2}} + \frac{g^2\mu^2}{32\pi^2}\int_{4M^2}^{\infty} dq^2\sqrt{1-\frac{4M^2}{q^2}} \\
&\quad \cdot \frac{1}{\left[q^2-m_p^2\right]^2}\int \frac{d\vec{l}}{(2\pi)^3}\frac{1}{\sqrt{\vec{l}^2+q^2}} \\
&= -\frac{\mu^2 m_p^2 Z}{8\pi^2}\left(\frac{1}{\epsilon}+\frac{1}{2}-\frac{\gamma}{2}\right) - \frac{\mu^2 g^2}{128\pi^4}\int_{4M^2}^{\infty} dq^2 \\
&\quad \cdot \sqrt{1-\frac{4M^2}{q^2}}\frac{q^2}{\left[q^2-m_p^2\right]^2}\left(\frac{1}{\epsilon}+\frac{1}{2}-\frac{\gamma}{2}\right) + \\
&\quad \frac{\mu^2 m_p^2 Z}{(4\pi)^2}\ln\left(\frac{m_p^2}{4\pi\nu^2}\right) + \frac{\mu^2 g^2}{(4\pi)^4}\int_{4M^2}^{\infty} dq^2\sqrt{1-\frac{4M^2}{q^2}} \\
&\quad \cdot \frac{q^2}{\left[q^2-m_p^2\right]^2}\ln\left(\frac{q^2}{4\pi\nu^2}\right). \qquad (17)
\end{aligned}
$$

The integral over q^2 on the last line can't be expressed in terms of standard mathematical functions, so we will leave it untouched.

3.4 Comparison with the renormalization group equation

The vacuum diagram we calculated contains the only Feynman diagram at first order that contributes to the β-coefficient of the parameter m^2 in the scalar Yukawa theory. We will compare the expression for the vacuum diagram to the renormalization group equation of m^2. In equation (17) we can distinguish between two parts: a part that is multiplied by a pole $1/\epsilon$ and a part that is multiplied by a logarithmic term. The first part, which contains a pole, can be seen to be the integrated renormalization group equation of m^2 of the scalar Yukawa theory up to first order:

$$
\int dq^2\ \frac{dm^2(q^2)}{dq^2} = \int dt\ \frac{dm^2(t)}{dt} = \frac{1}{16\pi^2}\int dt\ \beta(m^2(t))\ , \qquad (18)
$$

where we used that $t = \frac{1}{2}\ln\left(q^2/\mu_0^2\right)$, as explained in section 2.5. The second part is some sort of 'altered' renormalization group equation. The vacuum diagram thus doesn't exactly equal the renormalization group equation, but contains an extra term that appears to be a tweaked version of the renormalization group equation.

The assumption behind the renormalization group equation is that the transition between the one-particle state and the multiparticle state is abrupt. In other words the onset of the first contribution to the β-function is represented

by a step function rather than a smooth function. It is assumed that if we are far away from this transition point, i.e. for $q^2 \to \infty$, the results are the same. But is this really the case? As we have the exact result for the β-function, we can compare the two to test this statement. In the limit $q^2 \to \infty$ the integrand accompanied by the pole in equation (17) becomes:

$$\sqrt{1-\frac{4M^2}{q^2}}\frac{q^2}{\left[q^2-m_p^2\right]^2} \to \frac{1}{q^2}\ .$$

We can now also calculate the integral over q^2:

$$\int_{4M^2}^{\infty} dq^2\ \frac{1}{q^2} = \left[\ln(q^2)\right]_{4M^2}^{\infty}\ .$$

To test the statement, let's compare the integrands and full expressions with some graphs. We define the following functions to compare:

$$f(q^2) = \theta(q^2-4M^2)\frac{\mu^2 g^2}{128\pi^4}\sqrt{1-\frac{4M^2}{q^2}}\frac{q^2}{\left[q^2-m_p^2\right]^2}\ ,$$

$$g(q^2) = \theta(q^2-4M^2)\frac{\mu^2 g^2}{128\pi^4}\frac{1}{q^2}\ ,$$

$$F(S) = \frac{\mu^2 m_p^2 Z}{8\pi^2} + \theta(S-4M^2)\frac{\mu^2 g^2}{128\pi^4}\int_{4M^2}^{S} dq^2\sqrt{1-\frac{4M^2}{q^2}}\frac{q^2}{\left[q^2-m_p^2\right]^2}\ ,$$

$$G(S) = \frac{\mu^2 m_p^2 Z}{8\pi^2} + \theta(S-4M^2)\frac{\mu^2 g^2}{128\pi^4}\left[\ln(q^2)\right]_{4M^2}^{S}\ .$$

Scenario 1: $m_p \sim 2M$

Input (in arbitrary mass units): $M = 27, m_p = 50, \mu = 1, Z = 1, \sqrt{\frac{g^2}{4\pi}} \equiv \sqrt{\alpha} = \sqrt{150}$. Notice that we made sure that $m_p < 2M$, because of the stable particle condition. The coupling constant g has mass dimension 1, so we gave it a mass-like value. Figure 6 shows the functions $f(q^2)$ and $g(q^2)$, whereas Figure 7 shows the difference between them. For $m_p \sim 2M$ the exact function $f(q^2)$ lies above the approximate function $g(q^2)$. The square root and m_p^2 in $f(q^2)$ play a role at smaller energies. The square root gives rise to a dampening effect, whereas the fraction containing m_p^2 leads to a peaking effect. For larger energies the two functions approach each other, as expected. Figure 8 depicts the functions $F(S)$ and $G(S)$ and Figure 9 depicts the relative difference between the two. The deviation of the approximate function from the exact function seems to stabilize at around 1.2%.

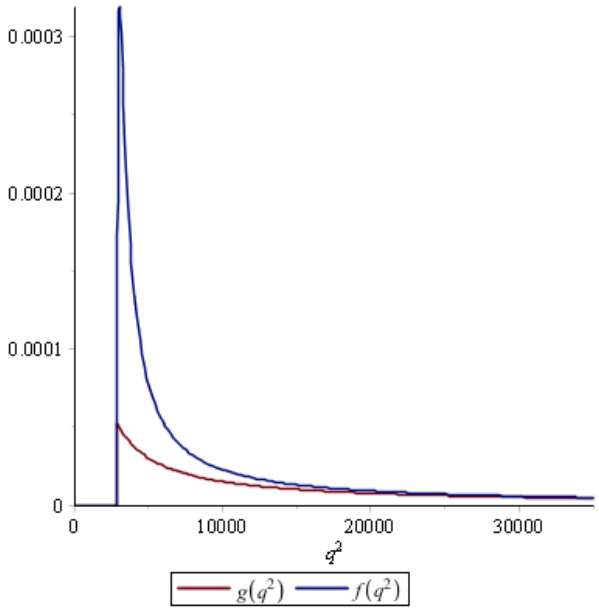

Figure 6: Plot of $f(q^2)$ and $g(q^2)$ for $M = 27$ and $m_p = 50$

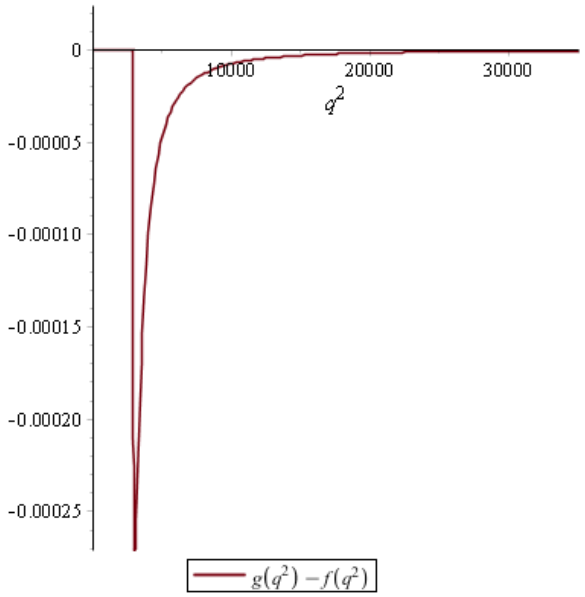

Figure 7: Plot of $g(q^2) - f(q^2)$ for $M = 27$ and $m_p = 50$

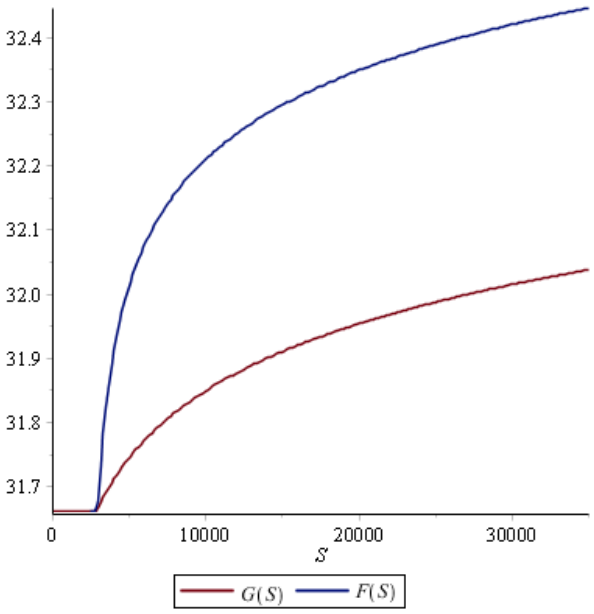

Figure 8: Plot of $F(S)$ and $G(S)$ for $M = 27$ and $m_p = 50$

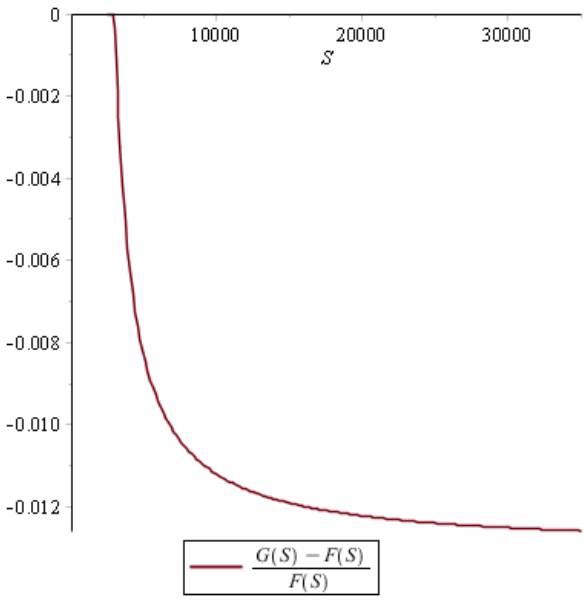

Figure 9: Plot of $\frac{G(S)-F(S)}{F(S)}$ for $M = 27$ and $m_p = 50$

Scenario 2: $m_p \ll 2M$

Input (in arbitrary mass units): $M = 500, m_p = 50, \mu = 1, Z = 1, \sqrt{\frac{g^2}{4\pi}} \equiv \sqrt{\alpha} = \sqrt{150}$. Figure 10 shows the functions $f(q^2)$ and $g(q^2)$ and Figure 11 shows the difference between the two. For $m_p \ll 2M$ the exact function lies beneath the approximate function. We can again observe the effects of the square root and fraction containing m_p^2. For larger energies the two functions approach each other again. Figure 12 shows the functions $F(S)$ and $G(S)$. Figure 13 shows the relative difference between $G(S)$ and $F(S)$. The difference seems to stabilize at around 0.27%.

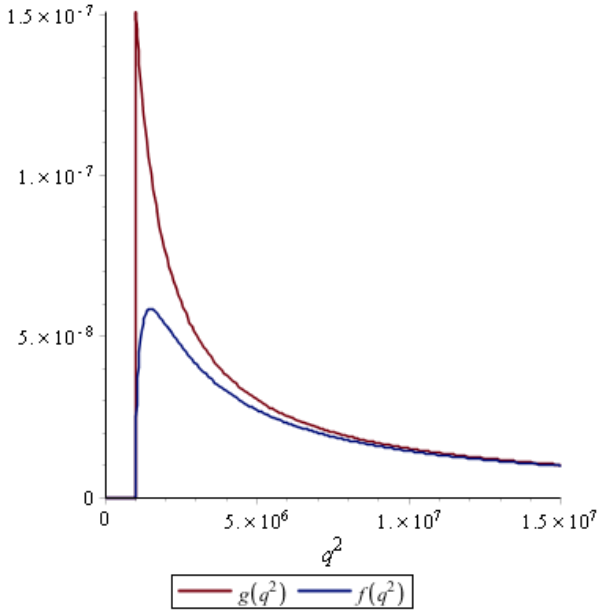

Figure 10: Plot of $f(q^2)$ and $g(q^2)$ for $M = 500$ and $m_p = 50$

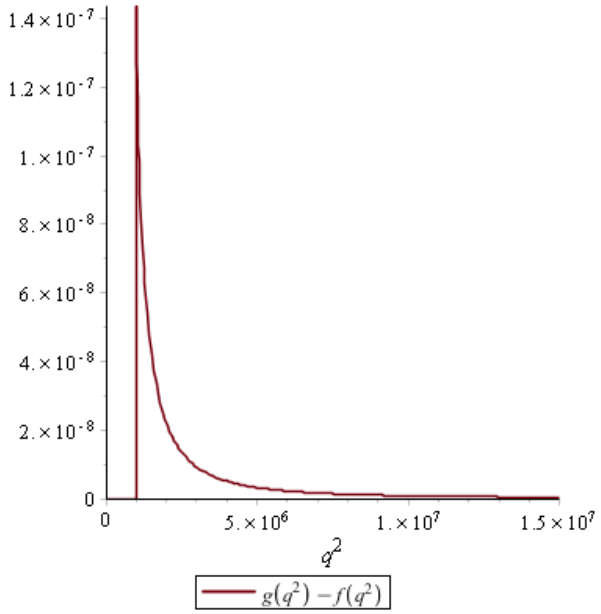

Figure 11: Plot of $g(q^2) - f(q^2)$ for $M = 500$ and $m_p = 50$

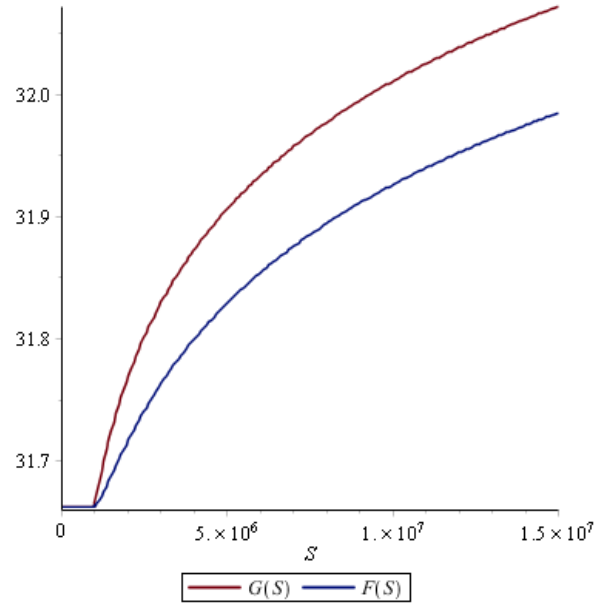

Figure 12: Plot of $F(S)$ and $G(S)$ for $M = 500$ and $m_p = 50$

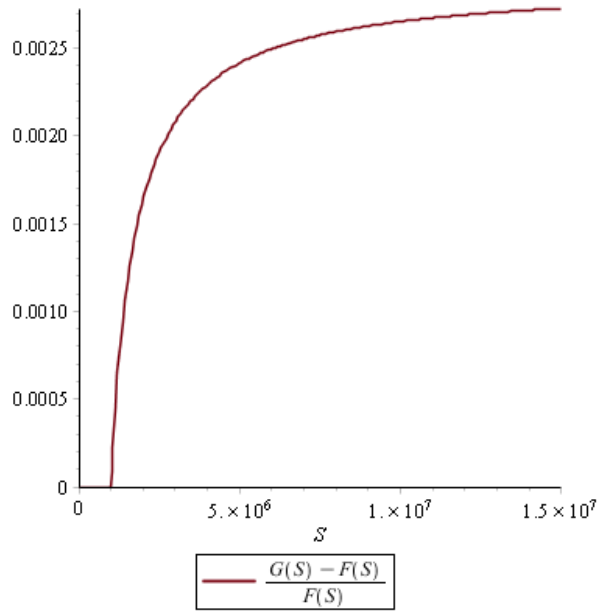

Figure 13: Plot of $\frac{G(S)-F(S)}{F(S)}$ for $M = 500$ and $m_p = 50$

This time we compared the approximated renormalization group equation to the exact one. We can do the same for the 'altered' renormalization group equation; the second part of equation (17). It is discussed in the Appendix.

4 Conclusion and outlook

The goal of our research was to investigate if there is a link between a vacuum diagram and the renormalization group equation. Thereby we were interested in the consequences of neglecting transitions in the renormalization group equation. We used the scalar Yukawa theory to answer our research questions and calculated the vacuum diagram belonging to the $\mu^2\phi^\dagger\phi$ term up to first order in perturbation theory.

We compared the expression for the vacuum diagram to the renormalization group equation of m^2. The expression consisted of two parts. The part multiplied by the pole $1/\epsilon$ was seen to be the integrated renormalization group equation of m^2 of the scalar Yukawa theory up to first order. The other part, containing an additional logarithmic term, looks like some 'altered' renormalization group equation. The vacuum diagram thus doesn't exactly equal the renormalization group equation, but contains an extra term.

Next we tested the assumption that the transition between the one-particle state and the multiparticle state can be neglected in the renormalization group equation. For that purpose we compared the exact expression of the renormalization group equation to the approximated version for $q^2 \to \infty$. For $m \sim 2M$ the difference between the two stabilizes at around 1.2%. For $m \ll 2M$ this is around 0.27%. During our calculation we only crossed one threshold at 1-loop order. If one crosses multiple thresholds the deviations will be summed. Such a correction could affect the renormalization group evolution in a noticeable way, in particular in more realistic models with cancellations between bosonic and fermionic loop effects. An example of a future study along this line could be the Standard Model Higgs self-coupling λ, which flirts with zero at high energies.

Of course the scalar Yukawa theory we used is just a toy model; a simplification of the Yukawa theory. The two theories differ by spin aspects and the dimension of the coupling constant. Moreover we assumed the particles to be stable, whereas many particles in the Standard Model are unstable. These simplifications enabled us to perform the calculation. We will leave it to follow-up research to remove the simplifications one by one. Another subject for further research is the renormalization of the μ^2 parameter, which we omitted since it would be meaningless in our toy model.

References

[1] W. Beenakker, 'Reader for the course Quantum Field Theory.' `http://www.hef.ru.nl/~wimb/dictaat_QFT.pdf`, 2015-2016.

[2] S.E. Rugh and H. Zinkernagel, *The Quantum vacuum and the Cosmological Constant Problem, Stud.Hist.Philos.Mod.Phys.* **33** (2002) 663705, [arXiv:0012253].

[3] A.N. Schellekens, 'Beyond the Standard Model.' `http://www.nikhef.nl/~t58/BSM.pdf`, February, 2016.

[4] S. Lepoeter, 'Properties of the vacuum.' August, 2014.

[5] I. van Vulpen, 'The Standard Model Higgs Boson.' `https://www.nikhef.nl/~ivov/HiggsLectureNote.pdf`, 2013-2014.

[6] M.E. Peskin and D.V. Schroeder, *An introduction to Quantum Field Theory.* Westview press, 1995.

[7] W.J.P. Beenakker, 'Electroweak corrections: techniques and applications.' 1989.

[8] E.M. Stein and R. Shakarchi, *Complex analysis.* Princeton university press, 2003.

A 'Altered' renormalization group equation

In section 3.4 we compared the approximated renormalization group equation to the exact one. This appendix discusses the same procedure for the 'altered' renormalization group equation; the second part of equation (17). In the limit $q^2 \to \infty$ the integrand containing a logarithm in equation (17) becomes:

$$\sqrt{1-\frac{4M^2}{q^2}}\frac{q^2}{\left[q^2-m_p^2\right]^2}\ln\left(\frac{q^2}{4\pi\nu^2}\right) \to \frac{1}{q^2}\ln\left(\frac{q^2}{4\pi\nu^2}\right).$$

We can now also calculate the integral over q^2:

$$\int_{4M^2}^{\infty} dq^2 \frac{1}{q^2}\ln\left(\frac{q^2}{4\pi\nu^2}\right) = \left[\frac{1}{2}\ln^2\left(\frac{q^2}{4\pi\nu^2}\right)\right]_{4M^2}^{\infty}.$$

Let's compare the integrands and full expressions with some graphs on the basis of the following functions:

$$\begin{aligned}
f(q^2) &= \theta(q^2-4M^2)\frac{g^2\mu^2}{(4\pi)^4}\sqrt{1-\frac{4M^2}{q^2}}\frac{q^2}{\left[q^2-m_p^2\right]^2}\ln\left(\frac{q^2}{4\pi\nu^2}\right),\\
g(q^2) &= \theta(q^2-4M^2)\frac{g^2\mu^2}{(4\pi)^4}\frac{1}{q^2}\ln\left(\frac{q^2}{4\pi\nu^2}\right),\\
F(S) &= \frac{m_p^2\mu^2}{(4\pi)^2}\ln\left(\frac{m_p^2}{4\pi\nu^2}\right) + \theta(S-4M^2)\frac{g^2\mu^2}{(4\pi)^4}\int_{4M^2}^{S} dq^2\\
&\quad\cdot\sqrt{1-\frac{4M^2}{q^2}}\frac{q^2}{\left[q^2-m_p^2\right]^2}\ln\left(\frac{q^2}{4\pi\nu^2}\right),\\
G(S) &= \frac{m_p^2\mu^2}{(4\pi)^2}\ln\left(\frac{m_p^2}{4\pi\nu^2}\right) + \theta(S-4M^2)\frac{g^2\mu^2}{(4\pi)^4}\left[\frac{1}{2}\ln^2\left(\frac{q^2}{4\pi\nu^2}\right)\right]_{4M^2}^{S}.
\end{aligned}$$

Scenario 1: $m_p \sim 2M$

Input (in arbitrary mass units): $M = 27, m_p = 50, \mu = 1, \nu = 1, Z = 1, \sqrt{\frac{g^2}{4\pi}} \equiv \sqrt{\alpha} = \sqrt{150}$. Figure 14 shows the functions $f(q^2)$ and $g(q^2)$, whereas Figure 15 shows the difference between them. For $m_p \sim 2M$ the exact function $f(q^2)$ lies above the approximate function $g(q^2)$. For larger energies the two functions approach each other. The qualitative behaviour of the graphs is similar to the ones in section 3.4. Figure 16 depicts the functions $F(S)$ and $G(S)$ and Figure 17 depicts the relative difference between the two. The deviation of the approximate function from the exact function seems to stabilize at around 1.4%.

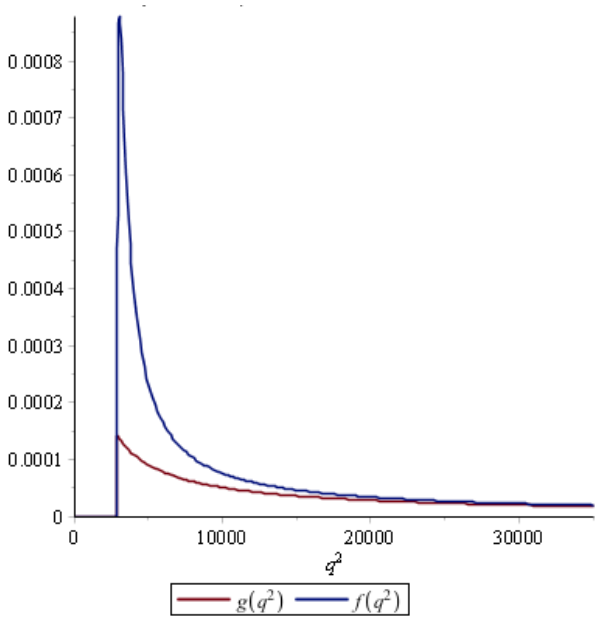

Figure 14: Plot of $f(q^2)$ and $g(q^2)$ for $M = 27$ and $m_p = 50$

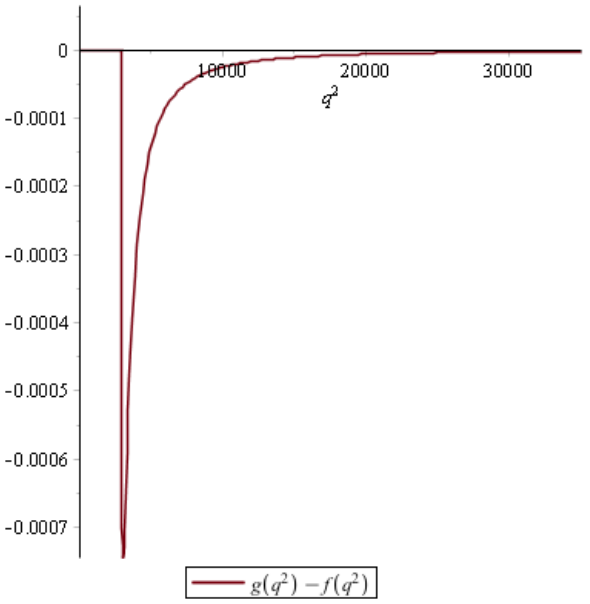

Figure 15: Plot of $g(q^2) - f(q^2)$ for $M = 27$ and $m_p = 50$

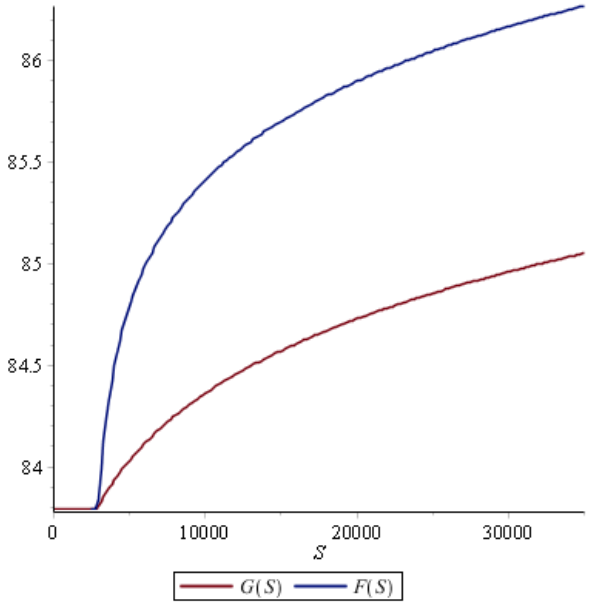

Figure 16: Plot of $F(S)$ and $G(S)$ for $M = 27$ and $m_p = 50$

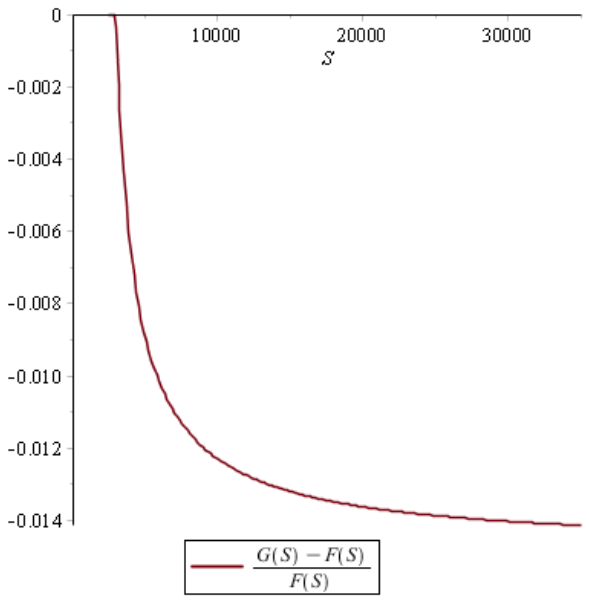

Figure 17: Plot of $\frac{G(S)-F(S)}{F(S)}$ for $M = 27$ and $m_p = 50$

Scenario 2: $m_p \ll 2M$

Input (in arbitrary mass units): $M = 500, m_p = 50, \mu = 1, \nu = 1, Z = 1, \sqrt{\frac{g^2}{4\pi}} \equiv \sqrt{\alpha} = \sqrt{150}$. Figure 18 shows the functions $f(q^2)$ and $g(q^2)$ and Figure 19 shows the difference between the two. For $m_p \ll 2M$ the exact function lies beneath the approximate function. For larger energies the two functions approach each other again. Figure 20 shows the functions $F(S)$ and $G(S)$. Figure 21 shows the relative difference between $G(S)$ and $F(S)$. The difference seems to stabilize at around 0.6%. The deviation is larger than in the case without a logarithm, which was also true for scenario 1.

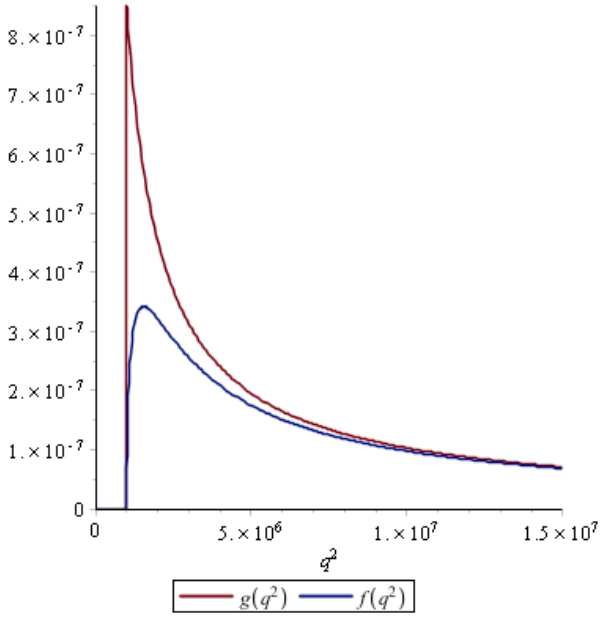

Figure 18: Plot of $f(q^2)$ and $g(q^2)$ for $M = 500$ and $m_p = 50$

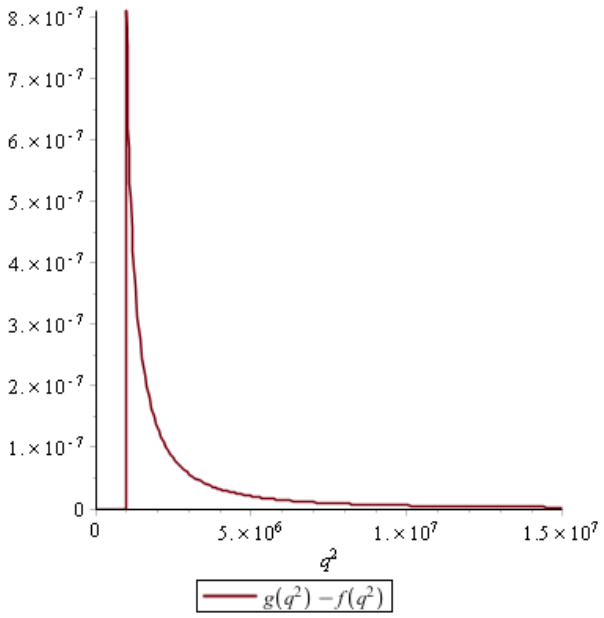

Figure 19: Plot of $g(q^2) - f(q^2)$ for $M = 500$ and $m_p = 50$

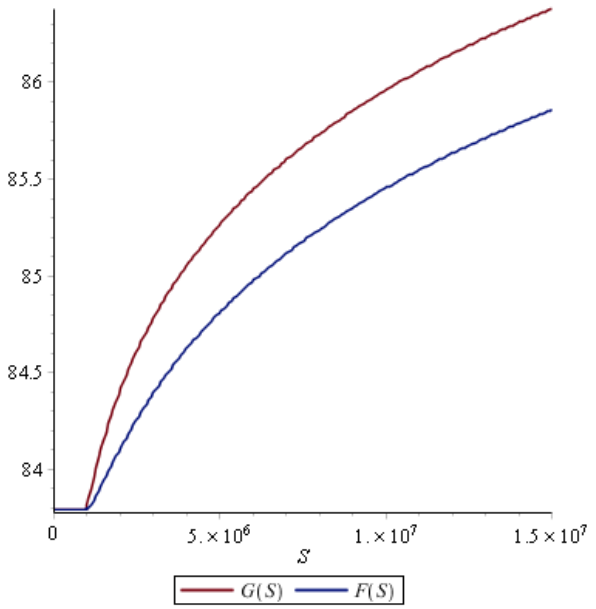

Figure 20: Plot of $F(S)$ and $G(S)$ for $M = 500$ and $m_p = 50$

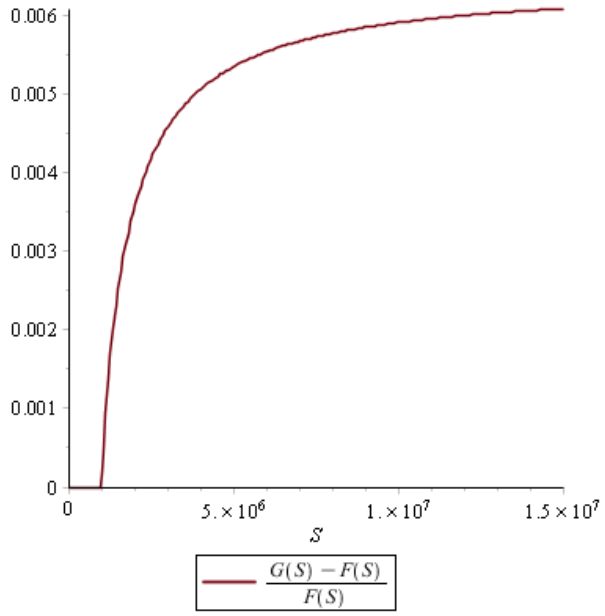

Figure 21: Plot of $\frac{G(S)-F(S)}{F(S)}$ for $M = 500$ and $m_p = 50$